Application of response surface methodology for optimization of methyl red adsorption by orange peels

B. Trifi[a,*], M.C. Bouallegue[a], I. Marzouk Trifi[b]

[a]INRAP, Laboratoire Matériaux, Traitement, et Analyse (LMTA), Institut National de Recherche et d'Analyse Physico-chimique (INRAP), Biotechpole Sidi Thabet, Tunisie, Tel./Fax: +21671537666; email: beyramtrifi@gmail.com (B. Trifi)
[b]U.R Traitement et Dessalement des Eaux, Faculté des Sciences de Tunis, Université de Tunis El Manar, 2092, Tunisie

ABSTRACT

Non-activated carbons prepared from orange peels were used as a low-cost adsorbent for the removal of an azo dye, methyl red. A methodology of surface response was used, this kind of designs estimate the coefficients of a quadratic polynomial mathematical model, whose essential interest is to be able to predict in any point of the experimental region, the values of the response. The effects of pH, stirring speed and adsorbent dose were investigated and the optimal conditions were ascertained by response surface methodology using Doehlert model. Results showed that stirring speed and pH were the main influent parameters on the removal of azo dye by adsorption onto non-activated carbon from orange peels. The statistical analysis of the experimental data assumes that they have a normal distribution. In this research, orange peels were demonstrated as a low-cost and efficient adsorbent for dye removal from aqueous solutions.

Keywords: Orange peels; Adsorption; Methyl red; Optimization; Response surface methodology

1. Introduction

Textile industry uses large volumes of water and generates important quantities of wastewater containing large amounts of dissolved dyes. About 50% of the dyes used are azo dyes [1,2]. These dyes can affect ecosystem and the aquatic flora and fauna. They can also cause health hazards because some of dyes are toxic and/or carcinogenic [3–5]. Some works report that ground water is also affected by these pollutants due to leaching from the soil [6,7].

Therefore, the toxicity and mass production of dyes leads to the necessity of treatment. Several processes are used to treat dyes laden wastewater such as biodegradation [8–11] or chemical and oxidative process [11–16]. However these techniques have limitations since the dyes are recalcitrant organic molecules, resistant to aerobic digestion, and stable to light and oxidizing agents [17].

Physicochemical processes are generally used for the wastewater color removal. These processes include electrocoagulation [18], coagulation/flocculation [11,19], membrane filtration [20,21] and adsorption [18,22]. The adsorption with activated carbon is one of the best techniques able to eliminate dye from aqueous effluent [17,23]. However, its widespread use is restricted due to its high cost [17,24]. In order to decrease the cost of treatment, development of both effective and low-cost adsorbents had been made from agriculture by-products and biomass such as rice husk [25], coffee residues [17], tea [26], coconut shell [27], corn cobs [28], olive stones [29], peanut hull [2], bagasse [30] and orange peels [7,31–33].

This paper reports on removal of methyl red, an azo dye, from aqueous solutions with non-activated carbon prepared from orange peels as potential low-cost adsorbents. Indeed, in front of the large production of oranges, a huge

* Corresponding author.

amount of orange peels is generated. In order to valorize this agricultural waste, it can be used as a biosorbent.

In this study, the preparation and characterization of the biosorbent were performed. Additionally, the batch adsorption behavior was investigated, studying the effect of pH, adsorbent dose and the stirring speed. The main scopes of this study are to obtain the optimum conditions for removal of methyl red using response surface methodology (RSM) approach.

2. Experimental

2.1. Preparation of the biosorbent

Oranges (*Citrus sinensis*) were purchased from a local fruit market, washed with tap water to eliminate dust and other residues and peeled. The orange peels were oven-dried at 60°C for 24 h. The dried peels were cut in small pieces and then crushed and further rinsed with warm water, dried again at 60°C for 24 h and finally sieved. The fraction of particle diameter between 500 and 1,000 μm was selected as biosorbent (abbreviated as OP).

2.2. Adsorbate and reagents

The synthetic wastewater was prepared with distilled water and azo dye methyl red (20 mg L^{-1}) as the model organic compound. Methyl red ($C_{15}H_{15}N_3O_2$, MW = 269.3, λ_{max} = 520 nm) was procured from Sigma-Aldrich (Tunisia). The structure of the dye is shown in Fig. 1. All reagents used were of analytical reagent grade.

2.3. Batch adsorption experiments

Adsorption experiments were carried out in a batch system using Erlenmeyer flasks under magnetic stirring. Afterwards, all samples were centrifuged and filtered then the concentration of dyes was calculated from the measured absorbance at the maximum absorption wavelength by means of an UV–Vis spectrophotometer (Thermo Scientific Evolution 201, Tunisia). Dye removal percentage was calculated as follows:

$$\text{Dye Removal}(\%) = \frac{C_0 - C_e}{C_0} \times 100 \qquad (1)$$

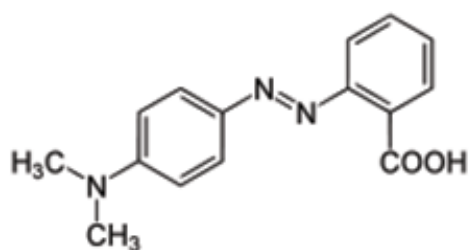with C_0 and C_e as the initial and equilibrium dye concentrations, respectively.

Fig. 1. Methyl red structure.

2.4. Characterization of the biosorbent

The total and individual amount of acidic functional groups and the total basic functional groups on the surface of the prepared OP were determined by titration following Boehm's method [34]. Average values expressed as millimole per gram of sample are reported. Identification of surface functionalities of OP was complementary conducted by Fourier transformed infrared (FTIR) spectroscopy. The spectra were recorded using a Bruker Platinum vertex 80 v spectrometer (Tunisia) within the range 600–4,000 cm^{-1}. The pH of point of zero charge (pH$_{pzc}$) for OP was evaluated [35]. Textural properties were assessed from N$_2$ adsorption isotherms with an automatic Micromeritics ASAP-2020 HV volumetric sorption analyzer (Tunisia). The Brunauer–Emmett–Teller (BET) surface area (S_{BET}) was determined by the standard BET procedure; total pore volume (V_t) was estimated from the amount of nitrogen adsorbed at the relative pressure of 0.95; mean pore width pore size (W) was determined with Barrett–Joyner–Halenda (BJH) model.

3. Results and discussion

3.1. Characterization of biosorbent

Chemical characteristics and textural properties of OP are presented in Table 1.

The pH$_{pzc}$ indicates the acidic nature of the orange peel–based adsorbent. It shows that the number of acid groups is close to that of basic groups. Moreover, it is noted that the majority of acidic groups are carboxylic having pKa (3–3.5) similar to pH$_{pzc}$.

Further insight into possible functional groups present on the surface of the prepared OP was obtained from the FTIR spectrum (Fig. 2). It displays a number of characteristic peaks. The broad, intense absorption peaks around 3,321 cm^{-1} are indicative of the absorption of water molecules, resulting from the O–H stretching mode of hydroxyl groups characteristic of adsorbed water, while the bands at 3,100 and 2,921 cm^{-1} were attributed to C–H interactions with the surface of the adsorbent. The peak at 1,735 cm^{-1} is due to the C=O stretching that can be attributed to the carboxylic

Table 1
Chemical characteristics and textural properties of OP

pH$_{pzc}$	3.5
Surface functional groups (mmol g^{-1})	
Total basics functional groups	2.44
Total and individual amount of acidic functional groups	2.41
Carboxyls	2.27
Lactones	0.12
Phenols	0.02
Textural properties	
S_{BET} (m^2 g^{-1})	2.6715
V_t (cm^3 g^{-1})	0.0014
W (Å)	21.0002
Vm	0.6138

Fig. 2. FTIR spectra of OP.

Fig. 4. Effect of stirring speed on the adsorption of MR.
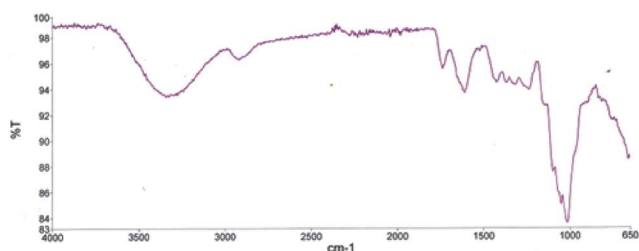
functions. The peak observed at 1,605 cm⁻¹ is due to the C=C stretching that can be attributed to the aromatic C–C bond. The peak around 1,357 cm⁻¹ is due to the symmetric bending of CH_3 and the peaks around 1,276 cm⁻¹ are due to C–O stretching of COOH.

The N_2 adsorption/desorption isotherms, illustrated in Fig. 3, shows a type I shape, according to Brunauer et al. [36] classification which is typical for microporous solid with a diameter less than 2 nm and covered by a monolayer. The presence of desorption hysteresis loop (H_3 type) is associated to slit-shaped pores [34,37]. Textural parameters, as evaluated from isotherms, are reported in Table 1. As can be observed, OP shows a low value of BET surface area (S_{BET} = 2.67 m² g⁻¹) and total pore volume (V_t = 0.0014 cm³ g⁻¹) in agreement with other experiments reported on the utilization of orange peels as biosorbent [32,33,38–40]. The mean pore width (W = 21 Å) confirms the microporous property of the OP determined by N_2 adsorption/desorption isotherms.

3.2. Preliminary study

During this part, we focused on the pre-optimization of the experimental parameters by varying a single parameter at each study.

3.2.1. Effect of stirring speed

In order to evaluate the influence of the stirring speed, 100 mL of 20 mg L⁻¹ MR solutions (pH = 6.5) with 1 g of OP were carried out with a variation of the stirring speed of 250 rpm up to 500 rpm. As shown in Fig. 4, dye removal
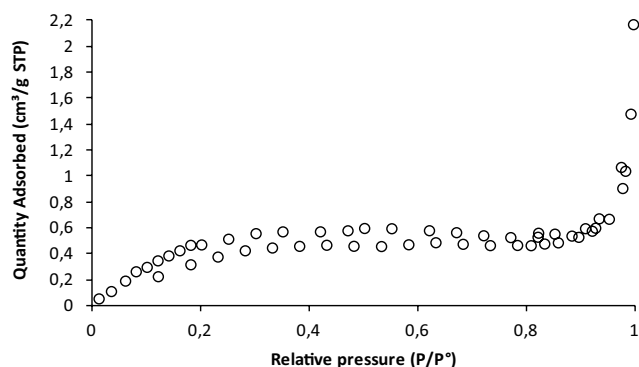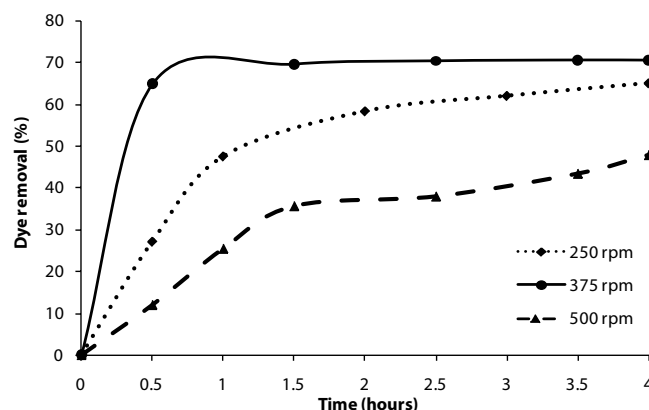
percentage reaches 70% in 30 min for a stirring speed equal to 375 rpm. However, the adsorption is slower for a speed of 250 rpm; it reaches 60% after 2 h. This can be explained by the fact that at low speeds, the contact time between the adsorbent and MR molecules is minimized. Otherwise, for a speed equal to 500 rpm, it is noted that the percentage of elimination varies slowly as a function of time to reach 50% after 4 h of contact. This can be explained by the fact that for high speeds, the turbulences generated within the medium do not favor the adsorption of the pollutant.

3.2.2. Effect of adsorbent dose

Doses of adsorbent from 0.25 to 1 g were brought into contact with 100 mL of 20 mg L⁻¹ MR solutions (pH = 6.5) with a stirring speed of 375 rpm. The results obtained are shown in Fig. 5. Usually the percentage of dye removal increases with increasing adsorbent dosage [41]. In fact, the increase in the mass of the adsorbent increases the total surface area and therefore the number of available adsorption sites and consequently the increase in the amount of the adsorbed dye. Thus the kinetics of adsorption strongly depends on the adsorbent dose. It should be noted that for 0.25 g per 100 mL we reached 65% after 150 min. For 0.5 g per 100 mL, we reached the same adsorption rate after 90 min

Fig. 3. N_2 adsorption/desorption isotherms of OP.
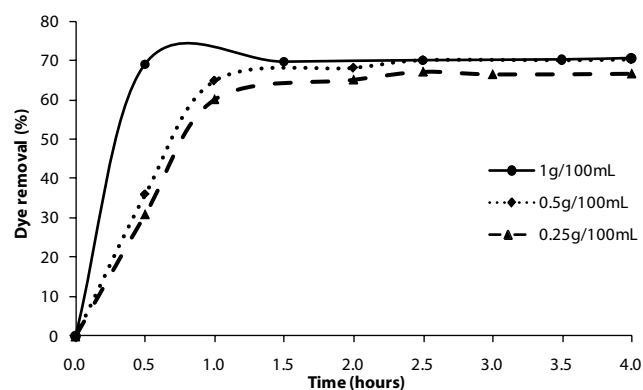

Fig. 5. Dye removal percentage vs. time at different adsorbent dose.

and for 1 g per 100 mL the same yield is achieved after only 30 min of contact time.

3.2.3. Effect of pH

The pH is a very important controlling parameter in the adsorption process especially for dye adsorption [31,41]. The effect of initial solution pH on the adsorption of MR from aqueous solution was investigated in the pH range between 3 and 11 (which was adjusted with 0.1 M HCl or 0.1 M NaOH using 100 mL of a 20 mg L^{-1} initial MR concentration and 1 g of OP for 2 h of contact (corresponding to the equilibrium time).

As shown in Fig. 6, a maximum of dye removal percentage is reached ($\approx$70%) for pH range between 6.5 and 7.5. Then it decreases at high pH solution (50% at pH = 11) even at low pH solution to reach 40% at pH = 2. Indeed, at high pH solution, the positive charge at the solution interface decreases and the adsorbent surface appears negatively char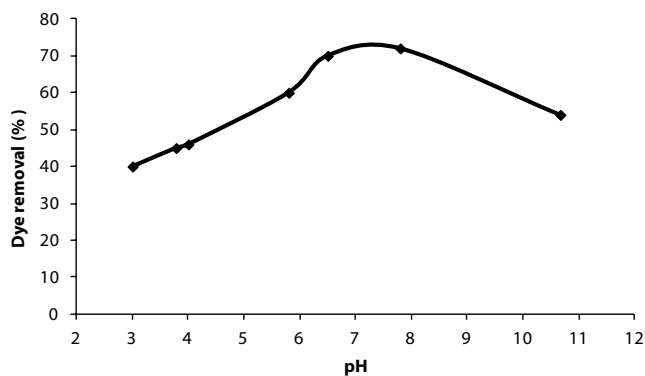ged because pH > pH$_{pzc}$ [31]. Lower adsorption at higher pH may be due to the abundance of OH$^-$ ions causing ionic repulsion between the negatively charged surface and the dye molecules charged negatively [31,41–43]. However, at a low pH solution, the positive charge on the solution interface will increase and the adsorbent surface appears to be positively charged (pH < pH$_{pzc}$) [43]. Consequently lower adsorption at acidic pH can be attributing to the competition between H$^+$ and MR molecule charged positively [31,41–43]. Similar type of behavior is also reported for the adsorption of dye with different adsorbents [30,42,44,45].

3.3. Optimization of experimental parameters

Optimization of experimental parameters is done by using RSM. The methodology is more economical and effective than the traditional "one-at-a-time" way [46]. It is a very effective and time saving model for studying the influence of experimental parameters on the response by significantly reducing the number of experiments and hence facilitating the optimum conditions considering interactions between experimental parameters [47]. In this study, RSM via Doehlert design was employed. This matrix makes it possible to estimate the coefficients of a second-order function, which is

Fig. 6. Effect of pH on the adsorption of MR after 2 h.

Table 2
Experimental values and coded levels of factors variables

Coded values of the variables	Variables	−1 (Low)	0	+1 (High)
X_1	U_1: pH	5	7	9
X_2	U_2: Adsorbent dose (g per 100 mL)	0.25	0.5	0.75
X_3	U_3: Stirring speed (rpm)	250	375	500

Table 3
Experimental and design matrix

N°	Doehlert design matrix			Experimental matrix			Dye removal percentage	
	X_1	X_2	X_3	U_1	U_2	U_3	Experimental Y Y_{exp}	Predicted Y Y_{pred}
1	1	0	0	9	0.500	375	30	37
2	−1	0	0	5	0.500	375	63	57
3	0.5	0.866	0	8	0.717	375	66	62
4	−0.5	−0.866	0	6	0.284	375	65	69
5	0.5	−0.866	0	8	0.284	375	55	53
6	−0.5	0.866	0	6	0.717	375	65	67
7	0.5	0.287	0.816	8	0.572	477	58	55
8	−0.5	−0.287	−0.816	6	0.428	273	28	31
9	0.5	−0.287	−0.816	8	0.428	273	22	17
10	0	0.577	−0.816	7	0.644	273	16	18
11	−0.5	0.287	0.816	6	0.572	477	57	62
12	0	−0.577	0.816	7	0.356	477	51	49
13	0	0	0	7	0.500	375	72	72

R^2 = 0.9535.

able to predict, at any point in the experimental domain, the values of the answer (*Y*) [47].

The calculated predictions must be as close as possible to the experimental values. The number of experiments for *k* factors is $N = k^2 + k + 1$. If *Y* (% removal after 2 h of contact) is the response, then mathematical relationship of the responses is:

$$Y = b_0 + b_1 X_1 + b_2 X_2 + b_3 X_3 + b_{11} X_1^2 + b_{22} X_2^2 + b_{33} X_3^2 + b_{12} X_1 X_2 + b_{13} X_1 X_3 + b_{23} X_2 X_3 \tag{2}$$

where b_0 intercept; b_1, b_2 and b_3 are linear coefficients; b_{11}, b_{22} and b_{33} are squared coefficients; b_{12}, b_{13} and b_{23} are the second-order interaction terms and X_1, X_2 and X_3 are the dimensionless coded factors of the following parameters studied pH, adsorbent dose and the stirring speed, respectively.

Experimental domain, deduced from the preliminary study (3.2) is illustrated in Table 2.

Doehlert design and experimental matrix for our three factors is then formed of 13 experiments as reported in Table 3.

Using the experimental results from Table 3, the second-order polynomial equation was fitted to the data appropriately and the equation is presented as follows:

$$Y = 72 - 10X_1 + 2.021X_2 + 20.412X_3 - 25.5X_1^2 - 3.834X_2^2 - 42.66X_3^2 + 6.3541X_1X_2 + 2.041X_1X_3 + 18.618X_2X_3 \tag{3}$$
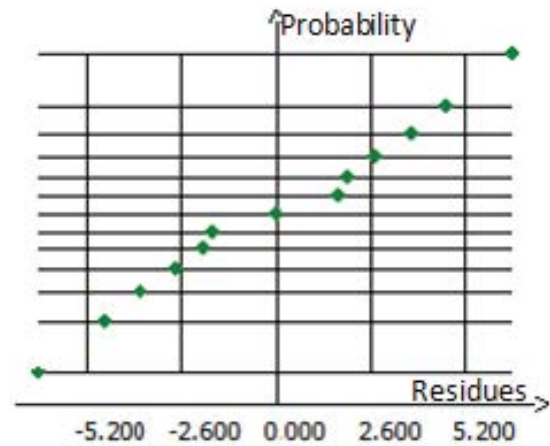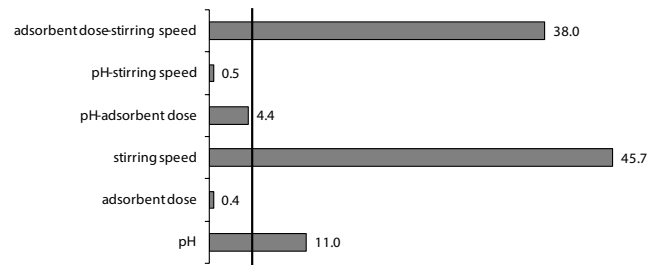

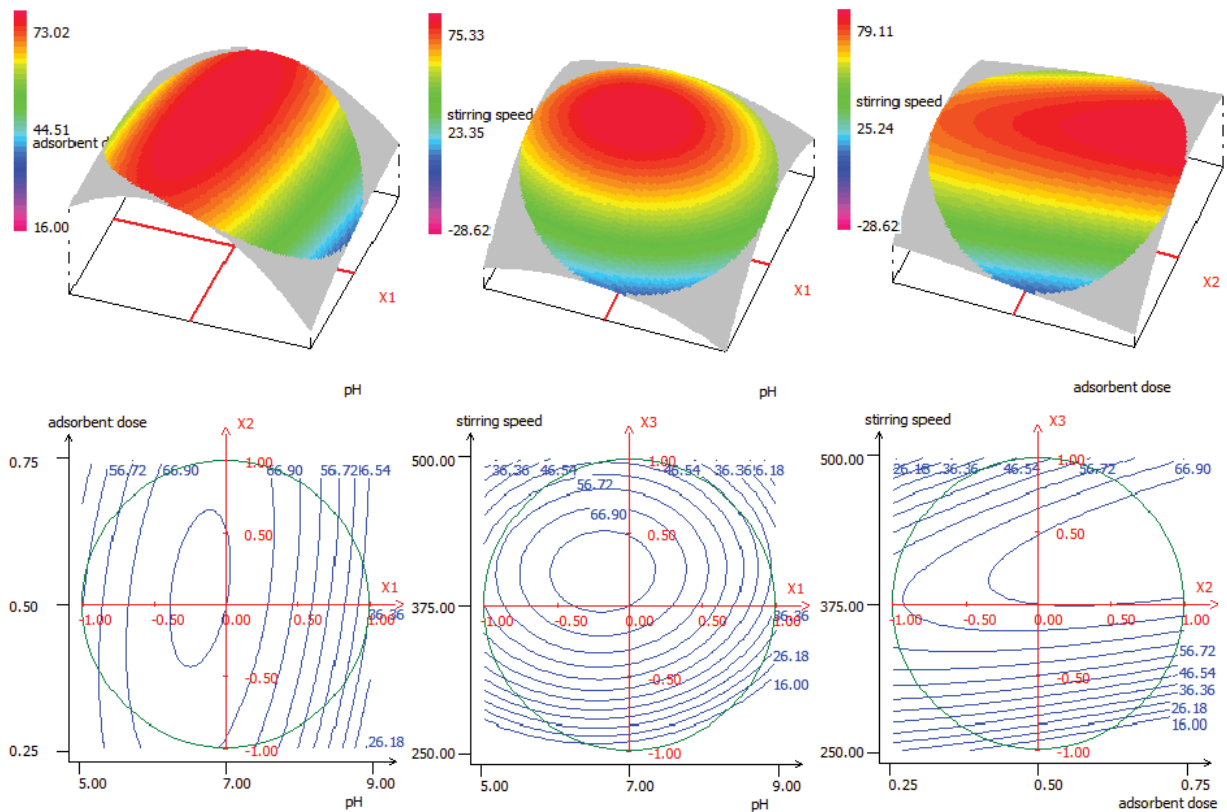Fig. 7. Normal plot of residues.

Fig. 8. Pareto effect of variables.

Fig. 9. Surface response.

Table 4
Results for validation

pH	7
Adsorbent dose	0.5 g/100 mL
Stirring speed	375 rpm
Y_1	72%
Y_2	70.6%
Y_3	71.7%
Y_{moy}	71.43%
Standard deviation	0.737
CV_R	1.03%

This model presents a good agreement among the model's predicted values and the experimental values ($R^2 = 0.9535$). Data obtained were also analyzed to check the normality of the residuals as shown in Fig. 7. From the plot, the data points lie reasonably close to a straight line; this shows that the developed model is adequate.

Fig. 8 shows the Pareto effects of factors and their interactions. It can be seen that the effect of pH is estimated at 11%. It is a significant factor (>5%) having a negative effect on the adsorption of methyl red. Moreover, the effect of the stirring speed is also a significant factor estimated at 45.7% ($b_3 = +20.4$) so an increase in stirring speed has a positive effect on the removal of the methyl red. The effect of the adsorbent dose–stirring speed interaction is the only significant interaction (38%). This effect is estimated at +18, thus these two parameters inter-react together to improve the adsorption of MR. Factors and their interaction having an estimated effect <5% are non-significant on the adsorption process.

In order to find the optimal conditions for the reaction, a response surface model was established (Fig. 9) by using NemrodW® program.

The maximum isoresponse plots ($Y = 72\%$) cross the origin of the axes. Thus the optimum of each factor is its central value ($X_i = 0$), namely a pH = 7; a biosorbent dose = 0.5 g per 100 mL of treated solution and a stirring speed = 375 rpm. In order to study the reproducibility of the optimized adsorption process, methyl red's adsorption was carried out three times under optimal conditions. Results are summarized in Table 4.

The repetition of the adsorption of methyl red on the bioadsorbent leads to an average equal to 71.4% and a $CV_R \approx 1\%$. This reproducibility coefficient is less than 5%, so the optimized adsorption process is considered reproducible. The results confirmed the validity of the model.

4. Conclusion

In this study, adsorption of methyl red onto non-activated carbon prepared from orange peels was studied. The Doehlert matrix has been used to build a mathematical model, which allowed establishing the optimal working conditions for the removal of dyes by adsorption. Results showed that for pH = 7, adsorbent dose = 0.5 g per 100 mL of treated solution and a stirring speed = 375 rpm for 2 h of contact and an initial concentration of dye = 20 mg L^{-1}, a removal dye efficiency = 72%

is reached. These results show good effectiveness of the use non-activated carbon prepared from orange peels as low-cost adsorbent for dye removal from aqueous solution.

References

[1] C. Bauer, P. Jacques, A. Kalt, Photooxidation of an azo dye induced by visible light Incident on the surface of TiO$_2$, J. Photochem. Photobiol., A, 140 (2001) 87–92.

[2] R. Gong, M. Li, C. Yang, Y. Suna, Removal of cationic dyes from aqueous solution by adsorption on peanut hull, J. Hazard. Mater., B121 (2005) 147–250.

[3] T. Zheng, T.R. Holford, S.T. Mayne, P.H. Owens, P. Boyle, B. Zhang, Use of hair colouring products and breast cancer risk: a case-control study in Connecticut, Eur. J. Cancer, 38 (2002) 1647–1652.

[4] G. Tezcanli-Guyer, N.H. Ince, Degradation and toxicity reduction of textile dyestuff by ultrasound, Ultrason. Sonochem., 10 (2003) 235–240.

[5] T. Sauer, G.C. Nero, H.J. Jose, R.F.P.M. Moreira, Kinetics of photocatalytic degradation of reactive dyes in a TiO$_2$ slurry reactor, J. Photochem. Photobiol., A, 149 (2002) 147–154.

[6] C. Namasivayam, S. Sumithra, Removal of direct red 12B and methylene blue from water by adsorption onto Fe (III)/Cr (III) hydroxide, an industrial solid waste, J. Environ. Manage., 74 (2005) 207–215.

[7] A. Khaled, A. El Nemr, A. El-Sikaily, O. Abdelwahab, Treatment of artificial textile dye effluent containing Direct Yellow 12 by orange peel carbon, Desalination, 238 (2009) 210–232.

[8] H. Ali, Biodegradation of synthetic dyes—a review, Water Air Soil Pollut., 213 (2010) 251–273.

[9] P.A. Joshi, S. Jaybhaye, K. Mhatre, Biodegradation of dyes using consortium of bacterial strains isolated from textile effluent, Eur. J. Exp. Biol., 5 (2015) 36–40.

[10] H. Lade, A. Kadam, D. Paul, S. Govindwar, Biodegradation and detoxification of textile azo dyes by bacterial consortium under sequential microaerophilic/aerobic processes, Exp. Clin. Sci. J., 14 (2015) 158–174.

[11] V. López-Grimau, M. Vilaseca, C. Gutiérrez-Bouzán, Comparison of different wastewater treatments for colour removal of reactive dye baths, Desal. Wat. Treat., 57 (2016) 2685–2692.

[12] F.N. Chianeh, J.B. Parsa, Decolorization of azo dye C.I. Acid Red 33 from aqueous solutions by anodic oxidation on MWCNTs/Ti electrodes, Desal. Wat. Treat., 57 (2016) 20574–20581.

[13] M.A. Oturan, J.J. Aaron, Advanced oxidation processes in water/wastewater treatment: principles and applications. A review, Crit. Rev. Env. Sci. Technol., 44 (2014) 2577–2641.

[14] W. Yang, H. Zhou, N. Cicek, Treatment of organic micropollutants in water and wastewater by UV-based processes: a literature review, Crit. Rev. Env. Sci. Technol., 44 (2014) 1443–1476.

[15] S.A. Kosa, N.M. Al-sebaii, I.H. Abd El Maksod, E.Z. Hegazy, New method for removal of organic dyes using supported iron oxide as a catalyst, J. Chem., 2016 (2016) 1–9.

[16] S. Atalay, G. Ersöz, Advanced Oxidation Processes for Removal of Dyes from Aqueous Media, S.K. Sharma FRSC Eds., Green Chemistry for Dyes Removal from Wastewater: Research Trends and Applications, John Wiley & Sons, Inc., Hoboken, NJ, USA, 2015.

[17] G.K. Kyzas, N.K. Lazaridis, A. Ch. Mitropoulos, Removal of dyes from aqueous solutions with untreated coffee residues as potential low-cost adsorbents: equilibrium, reuse and thermodynamic approach, Chem. Eng. J., 189–190 (2012) 148–159.

[18] E. Bazrafshan, M.R. Alipour, A.H. Mahvi, Textile wastewater treatment by application of combined chemical coagulation, electrocoagulation, and adsorption processes, Desal. Wat. Treat., 57 (2016) 9203–9215.

[19] M.R. Gadekar, M.M. Ahammed, Coagulation/flocculation process for dye removal using water treatment residuals: modelling through artificial neural networks, Desal. Wat. Treat., 57 (2016) 26392–26400.

[20] C. Thamaraiselvan, M. Noel, Membrane processes for dye wastewater treatment: recent progress in fouling control, Crit. Rev. Env. Sci. Technol., 45 (2015) 1007–1040.

[21] P.S. Goh, B.C. Ng, W.J. Lau, A.F. Ismail, Inorganic nanomaterials in polymeric ultrafiltration membranes for water treatment, Sep. Purif. Rev., 44 (2015) 216–249.

[22] M.T. Yagub, T.K. Sen, S. Afroze, H.M. Ang, Dye and its removal from aqueous solution by adsorption: a review, Adv. Colloid Interface Sci., 209 (2014) 172–184.

[23] F. Derbyshire, M. Jagtoyen, R. Andrews, A. Rao, I. Martin-Gullon, E. Grulke, Carbon materials in environmental applications, Chem. Phys. Carbon, 27 (2001) 1–66.

[24] Y.S. Al-Degs, M.A.M. Khraisheh, S.J. Allen, M.N. Ahmad, Adsorption characteristics of reactive dyes in columns of activated carbon, J. Hazard. Mater., 165 (2009) 944–949.

[25] Y. Li, X. Zhang, R. Yang, G. Li, C. Hu, Removal of dyes from aqueous solutions using activated carbon prepared from rice husk residue, Water Sci. Technol., 73 (2016) 1122–1130.

[26] J.-j. Gao, Y.-b. Qin, T. Zhou, D.-d. Cao, P. Xu, D. Hochstetter, Y.-f. Wang, Adsorption of methylene blue onto activated carbon produced from tea (*Camellia sinensis* L.) seed shells: kinetics, equilibrium, and thermodynamics studies, J. Zhejiang Univ. SCIENCE B (J. Biomed. Biotechnol.), 14 (2013) 650–658.

[27] U.J. Etim, S.A. Umoren, U.M. Eduok, Coconut coir dust as a low cost adsorbent for the removal of cationic dye from aqueous solution, J. Saudi Chem. Soc., 20 (2016) 67–76.

[28] A.E. Ensuncho-Munoz, J.G. Carriazo, Characterization of the carbonaceous materials obtained from different agro-industrial wastes, Environ. Technol., 36 (2015) 547–555.

[29] R. Hazzaa, M. Hussein, Adsorption of cationic dye from aqueous solution onto activated carbon prepared from olive stones, Environ. Technol. Innovation, 4 (2015) 36–51.

[30] A. Abdullah, M. Salleh, M. Mazlina, M. Noor, M. Osman, R. Wagiran, S. Sobri, Azo dye removal by adsorption using waste biomass: sugarcane bagasse, Int. J. Eng. Technol., 2 (2005) 8–13.

[31] V.S. Munagapati, D.S. Kim, Adsorption of anionic azo dye Congo Red from aqueous solution by Cationic Modified Orange Peel Powder, J. Mol. Liq., 220 (2016) 540–548.

[32] M.E. Fernandez, B. Ledesma, S. Román, P.R. Bonelli, A.L. Cukierman, Development and characterization of activated hydrochars from orange peels as potential adsorbents for emerging organic contaminants, Bioresour. Technol., 183 (2015) 221–228.

[33] A. Khalfaoui, I. Bendjamaa, T. Bensid, A.H. Meniai, K. Derbal, Effect of calcination on orange peels characteristics: application of an industrial dye adsorption, Chem. Eng. Trans., 38 (2014) 361–366.

[34] M.E. Fernandez, G.V. Nunell, P.R. Bonelli, A.L. Cukierman, Activated carbon developed from orange peels: batch and dynamic competitive adsorption of basic dyes, Ind. Crops Prod., 62 (2014) 437–445.

[35] P.C.C. Faria, J.M.M. Órfão, M.F.R. Pereira, Adsorption of anionic and cationic dyes on activated carbons with different surface chemistries, Water Res., 38 (2004) 2043–2052.

[36] S. Brunauer, L.S. Deming, W.E. Deming, E. Teller, On a theory of the van der waals adsorption of gases, J. Am. Chem. Soc., 62 (1940) 1723–1732.

[37] Z. Hu, M.P. Srinivasan, Y. Ni, Novel activation process for preparing highly microporous and mesoporous activated carbons, Carbon, 39 (2001) 877–886.

[38] M. Thirumavalavan, Y.L. Lai, J.F. Lee, Fourier transform infrared spectroscopic analysis of fruit peels before and after the adsorption of heavy metal ions from aqueous solution, J. Chem. Eng. Data, 56 (2011) 2249–2255.

[39] N.C. Feng, X.Y. Guo, S. Liang, Enhanced Cu(II) adsorption by orange peel modified with sodium hydroxide, Trans. Nonferrous Met. Soc. China, 20 (2010) 146–152.

[40] S. Kamsonlian, S. Suresh, C.B. Majumder, S. Chand, Characterization of banana and orange peels: biosorption mechanism, Int. J. Sci. Technol. Manage., 2 (2011) 1–7.

[41] M.A.M. Salleh, D.K. Mahmoud, W.A.W. Abdul Karim, A. Idris, Cationic and anionic dye adsorption by agricultural solid wastes: a comprehensive review, Desalination, 280 (2011) 1–13.

[42] T. Santhi, S. Manonmani, T. Smitha, Removal of methyl red from aqueous solution by activated carbon prepared from the annona squmosa seed by adsorption, Chem. Eng. Res. Bull., 14 (2010) 11–18.

[43] A. Özcan, Ç. Ömeroglu, Y. Erdogan, A.S. Özcan, Modification of bentonite with a cationic surfactant: an adsorption study of textile dye Reactive Blue 19, J. Hazard. Mater., 140 (2007) 173–179.

[44] K. Tanzim, M. ZainalAbedin, A novel bioadsorbent for the removal of methyl red from aqueous solutions, J. Environ. Sci. Toxicol. Food Technol., 9 (2015) 87–91.

[45] T. Santhi, S. Manonmani, T. Smitha, D. Sugirtha, K. Mahalakshm, Uptake of cationic dyes from aqueous solution by bioadsorption onto granular *Cucumis sativus*, J. Appl. Sci. Environ. Sanitation, 4 (2009) 29–35.

[46] U.K. Garg, M.P. Kaur, D. Sud, V.K. Garg, Removal of hexavalent chromium from aqueous solution by adsorption on treated sugarcane bagasse using response surface methodological approach, Desalination, 249 (2009) 475–479.

[47] T. Lundstedt, E. Seifert, L. Abramo, B. Thelin, Å. Nyström, J. Pettersen, R. Bergman, Experimental design and optimization, Chemom. Intell. Lab. Syst., 42 (1998) 3–40.